

SUPPLEMENTARY MATERIAL

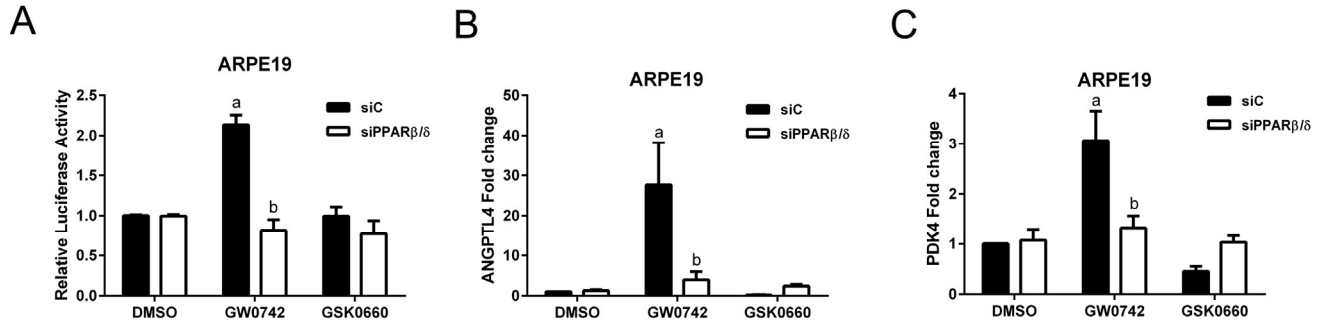


Figure S1. PPARβ/δ signaling pathway is functional in ARPE19 cells. (A) PPARβ/δ activity in ARPE19 cells transfected with the DR1 luciferase reporter and siC or siPPARβ/δ; cells were treated with PPARβ/δ agonist, GW0742 or antagonist, GSK0660 or DMSO as control ($n = 3$): a, $p < 0.05$ relative to DMSO treated cells; b, $p < 0.05$ relative to drug+siC treated cells ($p < 0.05$). Expression of (B) *ANGPTL4* and (C) *PDK4* mRNA in siC and siPPARβ/δ treated ARPE19 cells in response to GW0742, GSK0660, or DMSO as a control ($n = 3$); a: $p < 0.05$ relative to DMSO treated cells; b: $p < 0.05$ relative to drug+siC treated cells.

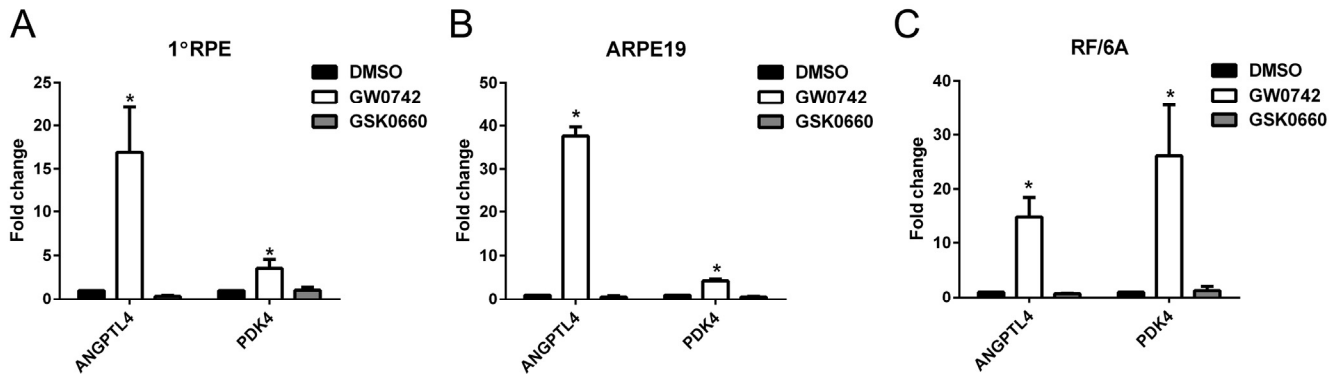


Figure S2. PPARβ/δ agonist and antagonist treatment of AMD vulnerable cells in the absence of transfection differentially effect receptor target gene expression. Human primary RPE (1°RPE); (A), ARPE19 (B), and RF/6A (C) cells were treated with GW0742 (10μM) and GSK0660 (10μM) for 24 hours, using DMSO as control. mRNA levels of the PPARβ/δ target genes *ANGPTL4* and *PDK4* were measured using qRT-PCR ($n=3$, $p<0.05$).

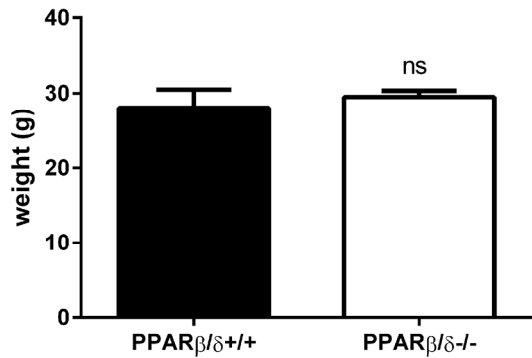


Figure S3. Comparison of body weights of age-matched *Pparβ/δ*^{+/+} and *Pparβ/δ*^{-/-} mice. Average weights of mice from *Pparβ/δ*^{+/+} (n=7) and *PPARβ/δ*^{-/-} (n=4) cohorts. (mean and S.E.M., ns: not significant).

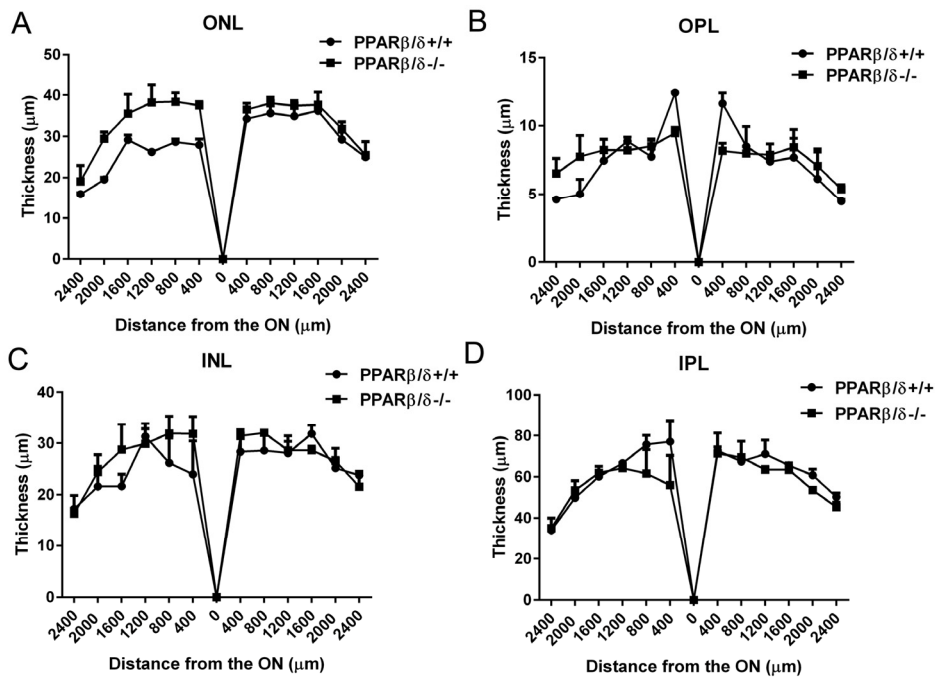
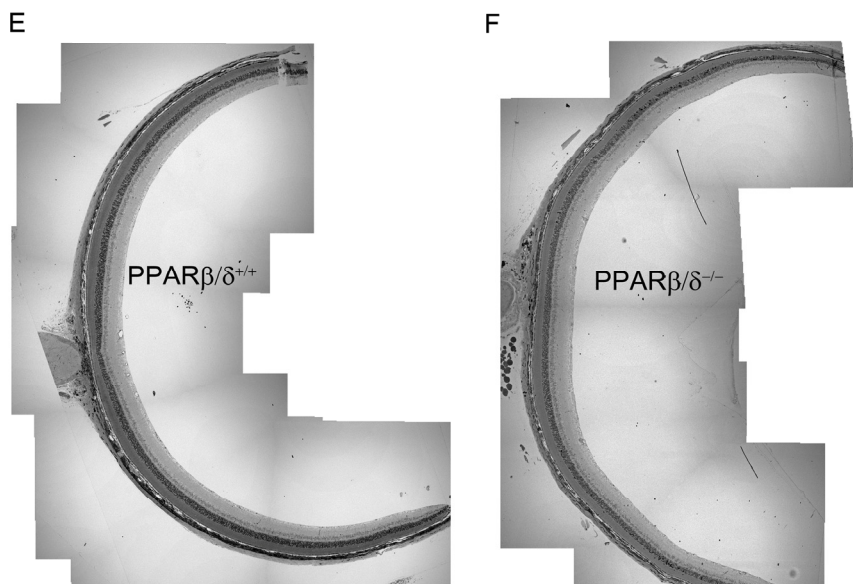


Figure S4. Quantification of thickness of retinal layers of *Pparβ/δ*^{+/+} and *Pparβ/δ*^{-/-} mice. Toluidine blue stained retinal sections were imaged from age matched *Pparβ/δ*^{+/+} (n=3) and *Pparβ/δ*^{-/-} (n=2) mice at 20X from end to end and images were tiled to create complete retinal section images. Six equidistant measurements of (A) outer nuclear layer (ONL) (B), outer plexiform layer (OPL), (C) inner nuclear layer (INL), and (D) inner plexiform layer (IPL) towards each end were made from the optic nerve. The thickness of these layers was plotted. Tiled images demonstrating overall retinal morphology of (E) *Pparβ/δ*^{+/+} and (F) *Pparβ/δ*^{-/-} mice.



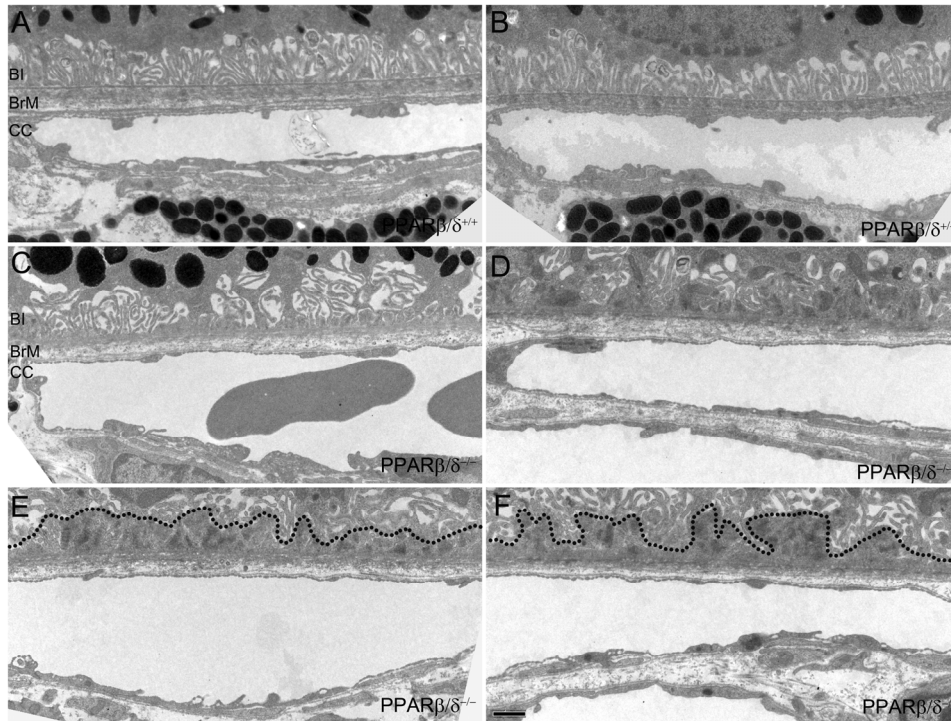


Figure S5. Genetic ablation of *Pparβ/δ* does not affect the integrity of the choriocapillaris. Morphology of the choriocapillaris was examined in electron micrographs. (A, B) Normal organization of the basal infolding of the RPE, Bruch's membrane (BrM) and fenestrated choriocapillaries (CC) in *Pparβ/δ*^{+/+} mice (n=4). (C, D, E, F) Sub-RPE deposits, disorganized basal infoldings of the RPE above morphologically normal looking fenestrated choriocapillaries. Apical limit of the sub-RPE deposits is outlined by a dotted line. N=8-14 images/mouse, n=4 mice/genotype were examined. Scale bar: 1 μm.

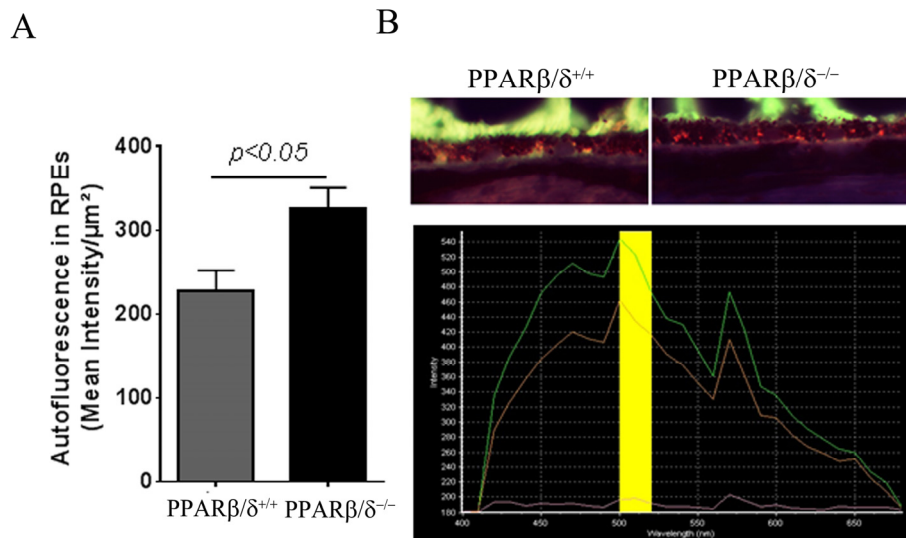


Figure S6. Genetic disruption of *Pparβ/δ* leads to lipofuscin accumulation *in vivo*. RPE autofluorescence was measured in *Pparβ/δ*^{+/+} and *Pparβ/δ*^{-/-} mice. (A) Quantification of lipofuscin autofluorescence in RPE from *Pparβ/δ*^{+/+} and *Pparβ/δ*^{-/-} mice. (B) Representative images and (C) plot of intensity versus wavelength of cryosections from *Pparβ/δ*^{+/+} and *Pparβ/δ*^{-/-} mice.

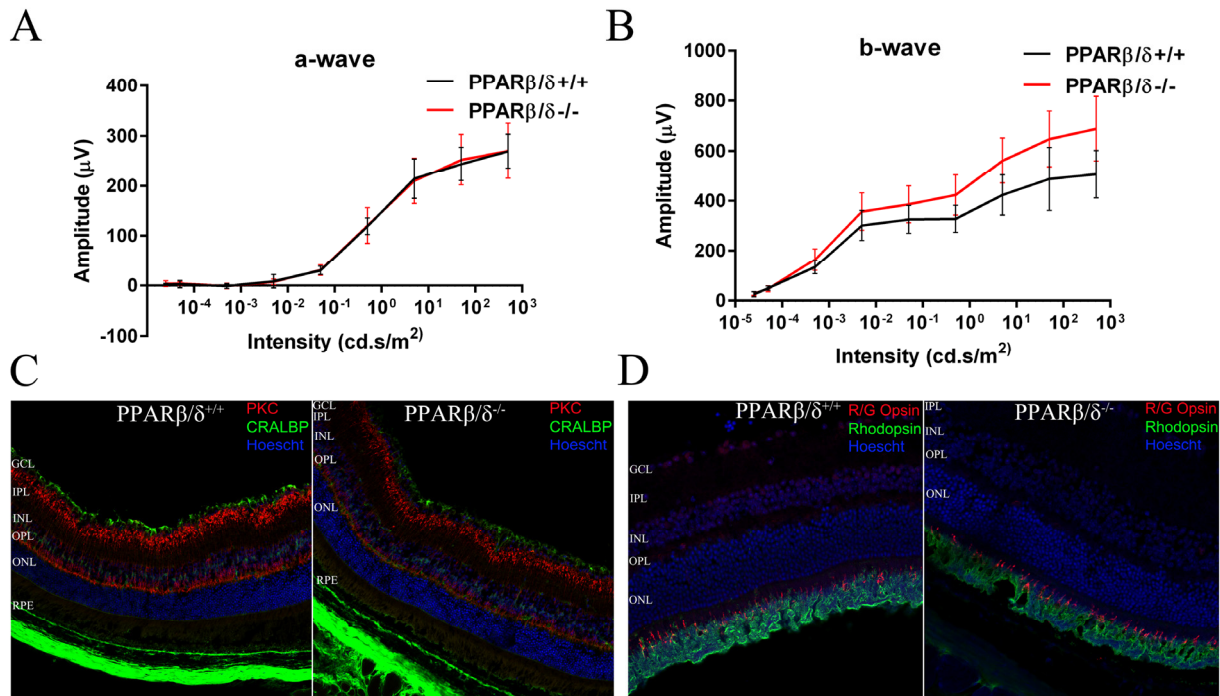


Figure S7. *Pparβ/δ*^{-/-} mice exhibit comparative ERG responses to age-matched *Pparβ/δ*^{+/+} mice. Averaged ERG responses in 14-16 month old dark-adapted *Pparβ/δ*^{+/+} (black) (n=5) and *Pparβ/δ*^{-/-} mice (red) (n=6). Plots of (A) dark-adapted a-wave amplitudes and (B) b-wave amplitudes as a function of flash intensity. Data points are mean and S.E.M. Immunolocalization of retinal markers in cryosections from 18-month old *Pparβ/δ*^{+/+} and *Pparβ/δ*^{-/-} mice probed with antibodies for (C) rod bipolar cells (PKCα, red) and Müller cells (CRALBP, green) and (D) red-green cone photoreceptors (R/G opsin, red) and rod photoreceptors (rhodopsin, green). Nuclei are stained with Hoescht (blue).

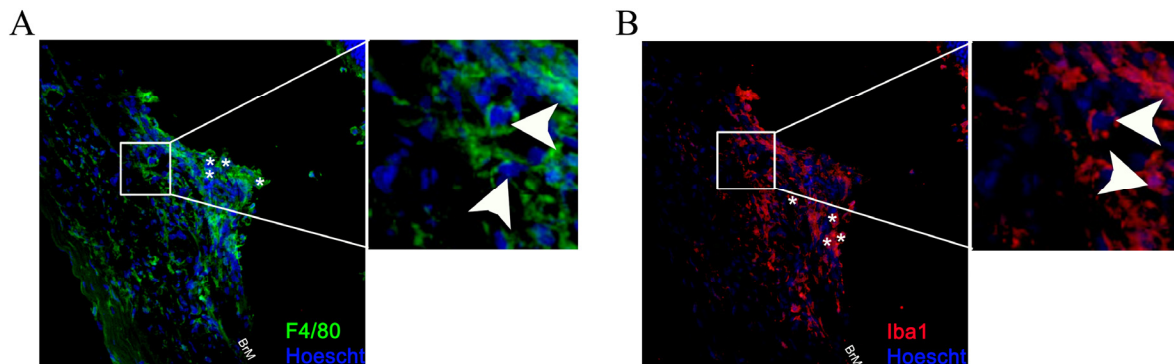


Figure S8. High magnification view of Iba1 and F4/80 staining in laser CNV lesions. Laser CNV lesions from *Pparβ/δ*^{-/-} mice display distinct F4/80 (green) (A) and Iba1 (red) (B) immunopositive cells. White arrowheads depict individual cells stained with F4/80 or Iba1. Asterisks mark some additional examples of positively stained cells.

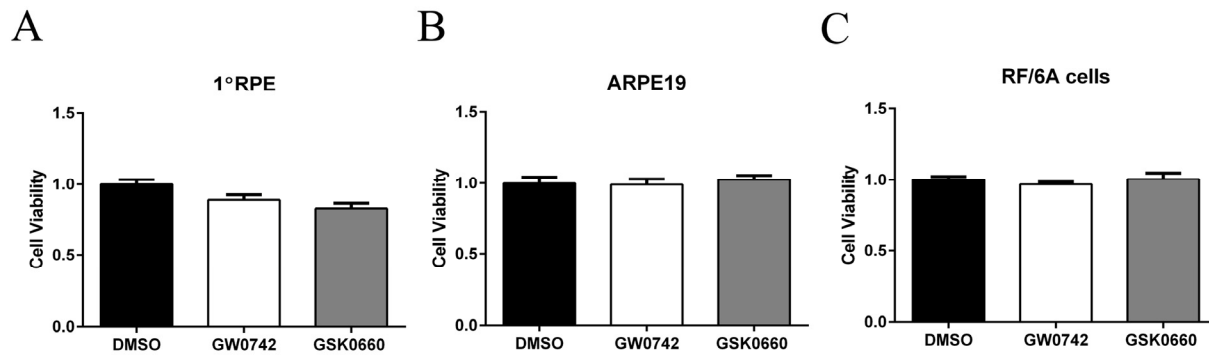


Figure S9. Ligand activation or pharmacological antagonism of PPAR β/δ does not affect cell viability in cell-culture models. Cell viability was measured after a 4 day treatment with the PPAR β/δ agonist, GW0742 or antagonist, GSK0660 in (A) primary RPE cells, (B) ARPE19 and (C) RF/6A cells.

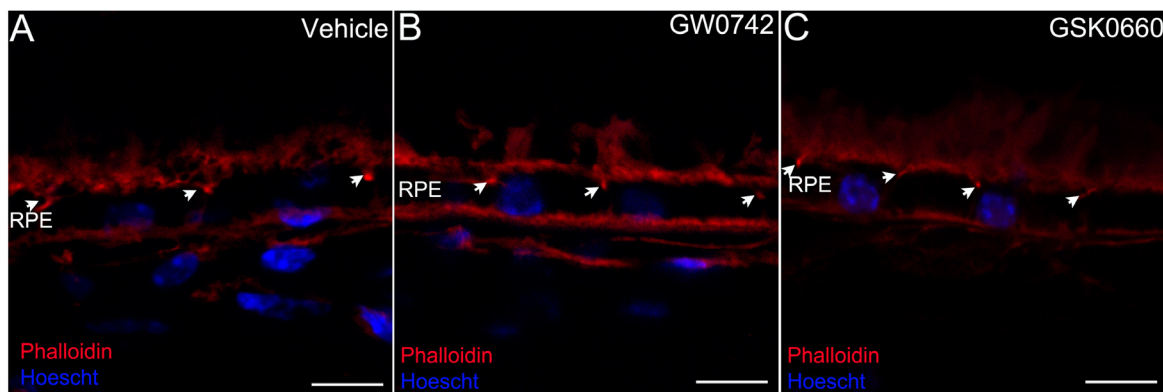


Figure S10. Ligand activation or pharmacological antagonism of PPAR β/δ does not affect RPE tight junctions *in vivo*. Localization of phalloidin (red) in cross-sections from mice treated with (A) vehicle control (1% DMSO in saline), (B) GW0742 (0.5mg/kg/day, i.p.), or (C) GSK0660 (1m/kg/day, i.p.). Apical localization is indicated by white arrows. Hoescht was used to stain nuclei.

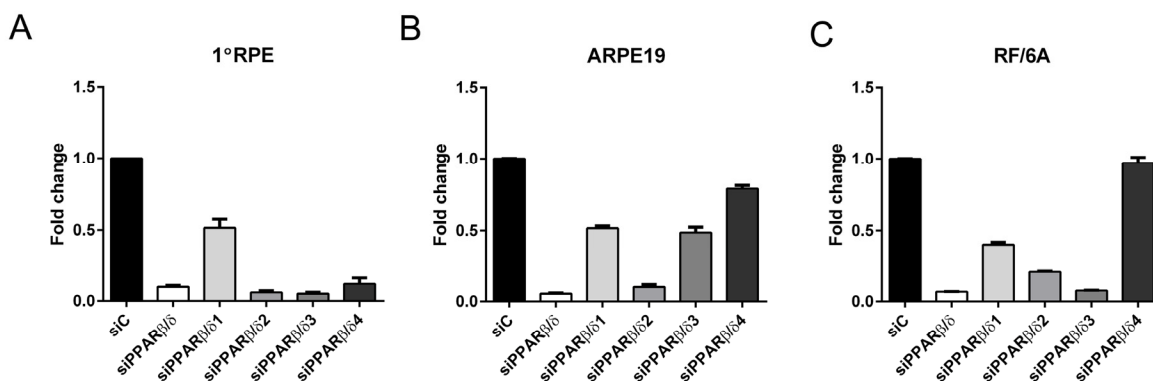


Figure S11. Validation of PPAR β/δ knockdown in cell-culture models. Multiple siRNAs targeting PPAR β/δ listed in Table S2 were tested in cell culture models used in this study. RT-PCR was used to measure the expression of PPAR β/δ mRNA levels 24 hours after siRNA transfection. Effect of siRNA transfection on PPAR β/δ gene expression in (A) primary RPE cells, (B) ARPE19 and (C) RF/6A cells. siC, control siRNA; siPPAR β/δ , PPAR β/δ siRNA.

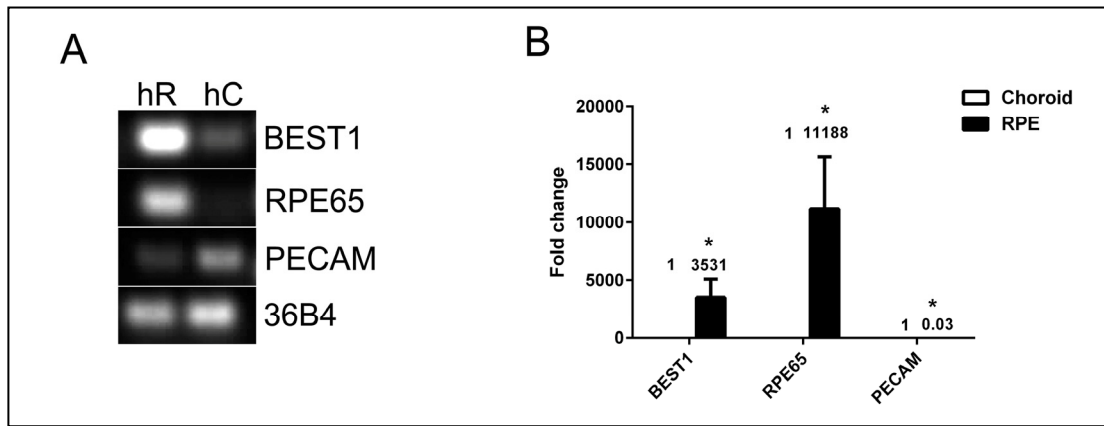


Figure S12. Freshly isolated RPE and choroid from human donor eyes have minimal cross contamination. mRNA expression of *BEST1*, *RPE65* and *PECAM* in freshly isolated RPE cells relative to freshly isolated choroidal cells (A, n=3, p<0.05), The mean fold change for each gene is depicted on the graph (B).

Table S1. List of drugs, concentrations, and sources.

Drugs	Concentration	Source
GW0742	10 μ M	Sigma-Aldrich
GSK0660	10 μ M	Sigma-Aldrich

Table S2. List of siRNAs.

siRNA	Company	Catalog#
siC	Qiagen	1027281
siPPAR β/δ	Dharmacon	L-003435-00-0005
siPPAR β/δ 1	Dharmacon	J-003435-06
siPPAR β/δ 2	Dharmacon	J-003435-07
siPPAR β/δ 3	Dharmacon	J-003435-08
siPPAR β/δ 4	Dharmacon	J-003435-09

Table S3. List of primers.

Gene	Primers	Sequence 5'→3' Human
36B4	Forward	GGACATGTTGCTGGCCAATAA
	Reverse	GGGCCCCGAGACCAGTGTT
ANGPTL4	Forward	GTCCACCGACCTCCCGTT A
	Reverse	CCTCATGGTCTAGGTGCTTGT
BEST1	Forward	AACTGAGCCTACCACACAACA
	Reverse	CGGATTCGACCTCCAAGCC
COLA1	Forward	TCACCAGGACAGAAGGGAAG
	Reverse	CTCTGGCACCTTTTGCTAGG
COL4A4	Forward	CTGGATTTGGAGAACGTACCG
	Reverse	TGATCCAATTCTGCCTGCAC
FN1	Forward	ATGATGAGGTGCACGTGTGT
	Reverse	CTCTTCATGACGCTTGTGGA
PDGFRB	Forward	AGCACCTTCGTTCTGACCTG
	Reverse	TATTCTCCCGTGTCTAGCCCA
PDK4	Forward	GGAGCATTCTCGCGCTACA
	Reverse	ACAGGCAATTCTTGTGCGAAA
PECAM1	Forward	AACAGTGTTGACATGAAGAGCC
	Reverse	TGTA AACAGCAGCAGTCATCCTT
PPARD	Forward	CCAACAGATGAAGACAGATGCA
	Reverse	CTGAACGCAGATGGACCTCTA
RPE65	Forward	CCTGCTGGTGGTTACAAGAAA
	Reverse	CCTGCCTGTTACATGAGCTGT
RXRA	Forward	GAGCCCAAGACCGAGACCTA
	Reverse	AGCTGTTTGTGCGCTGCTT
RXRB	Forward	AGCCCCAGATTA ACTCAACA
	Reverse	GATTGCACATAGCCGTTTGC
SERPINF1	Forward	TTCAAAGTCCCCGTGAACAAG
	Reverse	GAGAGCCCGGTGAATGATGG
TGFB1	Forward	CAATTCCTGGCGATACCTCAG
	Reverse	AGATAACCACTCTGGCGAGTC
VEGFA	Forward	AGGGCAGAATCATCACGAAGT
	Reverse	AGGGTCTCGATTGGATGGCA
VTN	Forward	CACTATGCCGGAGGATGAGT
	Reverse	TCAGGATTCCCTTTGGACTG

Table S4. List of drugs, concentrations, and sources.

Antibody/Stain	Source	Dilution
Apolipoprotein E (ApoE)	Millipore	1:1000
Collagen IV (COL4)	Millipore	1:30
CRALBP	Gift from John C Saari and Thermo Fisher	1:2500
F4/80	AbD Serotec	1:500
Fibronectin (FN1)	Abcam	1:100
Iba1 (Ionized calcium-binding adapter molecule 1)	WAKO	1:200
PKC α	Abcam	1:200
Red-Green Opsin	Millipore	1:1000
Rhodopsin	Abcam	1:1000
SV2	Hybridoma bank	1:200
Phalloidin Tetramethylrhodamine B isothiocyanate	Sigma	1:500

